SERPINA3K Protects against Oxidative Stress via Modulating ROS Generation/Degradation and KEAP1-NRF2 Pathway in the Corneal Epithelium

Tong Zhou,[1,3] *Rongrong Zong,*[1,3] *Zhoujing Zhang,*[1] *Chengpeng Zhu,*[1] *Fangyu Pan,*[1] *Xinye Xiao,*[1] *Zhen Liu,*[1] *Hui He,*[1] *Jian-xing Ma,*[2] *Zuguo Liu,*[*,1] *and Yueping Zhou*[*,1,3]

Purpose. We recently reported that SERPINA3K (SA3K), a member of the serine proteinase inhibitor (SERPIN) family, has antiangiogenic and anti-inflammatory activities. Here we investigated the antioxidant effects of SA3K in the corneal epithelium and the mechanism underlying its action.

Methods. We established the oxidative stress models induced by hydrogen peroxide (H_2O_2) in cultured human corneal epithelial (HCE) cells and in rat corneal epithelium in vivo. Cell viability, flow cytometry, and TUNEL analysis were conducted to detect viable cells and cell death; reactive oxygen species (ROS) and 3-Nitrotyrosine fluorescent assay was applied to measure ROS levels. Activity assay, immunostaining, Western blot, and quantitative RT-PCR were performed to analyze the factors of the ROS generation/degradation system and pathway.

Results. SA3K protected the HCE cells from H_2O_2-induced oxidative stress in a dose- and time-dependent manner. SA3K also significantly reduced the production of ROS. Regarding the mechanism underlying these effects, SA3K downregulated ROS generation by inhibiting NOX4 and upregulated ROS degradation by increasing the activity of superoxide dismutases and catalase. Furthermore, H_2O_2 induced activation of the Kelch-like ECH-associated protein 1 (KEAP1)/NF-E2–related factor-2 (NRF2) pathway, while SA3K inhibited H_2O_2-induced activation of KEAP1 and NRF2 and their downstream factors, including NAD(P)H quinone oxidoreductase and glutathione S-transferase. In the H_2O_2-induced rat corneal epithelium, SA3K alleviated the oxidative stress and downregulated NOX4 and NRF2.

Conclusions. Collectively, SA3K protects against oxidative stress by targeting the ROS generation/degradation system and modulating the KEAP1-NRF2 signaling pathway. (*Invest Ophthalmol Vis Sci.* 2012;53:5033–5043) DOI:10.1167/iovs.12-9729

It is known that the excess formation of reactive oxygen species (ROS) products, in a state of oxidative stress, contributes to the pathogenesis of multiple diseases, for example, neurodegenerative diseases, cancer, diabetes, and vascular disorders.[1–4] Oxidative stress also becomes an important target of some pharmacologic interventions.[5] These ROS products mainly include superoxide anion (O_2^-), hydroxyl radical (· OH), and hydrogen peroxide (H_2O_2). 3-Nitrotyrosine (3-NT) has also been considered a byproduct of ROS.[6] Oxidative stress is believed to play an important role in several ocular diseases including Fuchs' endothelial corneal dystrophy,[7–9] keratoconus, and others.[10] It has been reported that 3-NT is expressed in certain corneal diseases, such as keratoconus and Fuchs' corneal dystrophy.[6] In experimental research, H_2O_2, one of the main ROS products, has been often applied and investigated as a useful oxidative stress model.[5]

The NOX family of NADPH oxidase, a main ROS generation factor, has been intensively studied, since these components of the ROS system may play roles in the pathogenesis of diseases. Six NOX family members have been identified so far, namely, NOX1, NOX3, NOX4, NOX5, DUOX1, and DUOX2.[11–14] NOX4 is found in the macrophage at the start of inflammation and is believed to be involved in the generation of H_2O_2.[15,16]

There is a balance between ROS generation (pro-oxidants, i.e., NADPH oxidase) and ROS degradation (antioxidants, e.g., superoxide dismutases [SODs] and catalase) in the cells. Both excess of NADPH oxidase–derived ROS or dysfunction of antioxidant enzyme can result in an abnormal oxidative stress state.[17]

NF-E2–related factor-2 (NRF2) is a transcription factor.[18,19] Lately, the research on the function and mechanism of NRF2 has drawn a lot of attention and recently, suboptimal NRF2 function has been suggested to play a key role in some of the ocular diseases, namely Fuchs' endothelial corneal dystrophy.[10] When the cell is not under oxidative stress, NRF2 is bound to Kelch-like ECH-associated protein 1 (KEAP1), forming a structural complex, the KEAP1-NRF2 complex. KEAP1 inhibits the activity of NRF2 and accelerates the degradation of NFR2. The binding site of NRF2 to KEAP1has been identified.[20,21] When the cell is under the stimulation of oxidative stress, the KEAP1-NRF2 complex dissociates, leading to NRF2 accumulation in the cytoplasm and NRF2 translocation into the nucleus; this initiates phase 2 of the antioxidant response element (ARE) system, which plays an antioxidant role by activating the downstream antioxidant factor genes, such as quinone

From the [1]Eye Institute of Xiamen University, Fujian Provincial Key Laboratory of Ophthalmology and Visual Science, Xiamen, Fujian, China; and the [2]Department of Physiology, The University of Oklahoma Health Sciences Center, Oklahoma City, Oklahoma.

[3]These authors contributed equally to this work.

Supported by Natural Science Foundation of China Grant 81170818 (YZ) and Natural Science Foundation of Fujian Province of China Grant 2011J01255 (YZ).

Submitted for publication February 19, 2012; revised June 5, 2012; accepted June 19, 2012.

Disclosure: **T. Zhou**, None; **R. Zong**, None; **Z. Zhang**, None; **C. Zhu**, None; **F. Pan**, None; **X. Xiao**, None; **Z. Liu**, None; **H. He**, None; **J.-X. Ma**, None; **Z. Liu**, None; **Y. Zhou**, None

*Each of the following is a corresponding author: Yueping Zhou, Eye Institute and Xiamen Eye Center of Xiamen University, 422 South Siming Road, Xiamen, Fujian, China, 361005; ypzhou@yahoo.com.

Zuguo Liu, Eye Institute and Xiamen Eye Center of Xiamen University, 422 South Siming Road, Xiamen, Fujian, China, 361005; zuguoliu@xmu.edu.cn.

oxidoreductase (*NQO1*) and glutathione S-transferase (*GSTP*).[22–24] This signaling pathway is also called KEAP1-NRF2 or KEAP1-NRF2-ARE pathway.

SERPINA3K (SA3K), a member of the serine proteinase inhibitor (SERPIN) family, also known as kallikrein-binding protein, was first identified as a specific inhibitor of tissue kallikrein, as it specifically binds with tissue kallikrein to form a covalent complex and inhibits its proteolytic activities.[25] It is expressed in the liver, kidney, and ocular tissues. It has been recently shown that SA3K has antineovascularization, anti-inflammation, and antioxidative stress effects in the retina.[26–28] It has lately been reported that SA3K, as an inhibitor of Wnt pathway, plays a unifying role in its antiangiogenesis and anti-inflammatory effects.[29]

We have recently shown that SA3K has antiangiogenic and anti-inflammatory effects on the corneal injury.[30] To evaluate the antioxidant effect of SA3K in this present study, we examined the protective effects of SA3K against H_2O_2-induced oxidative stress and investigated its underlying mechanism on ROS signaling, by focusing on ROS generation, that is, NOX4, and ROS degradation, that is, SOD, catalase, as well as the KEAP1-NRF2 pathway and its downstream ARE family factors.

Materials and Methods

Materials

MTT [3-(4,5-dimethylthiazol-2-yl)-2,5-diphenyltetrazolium bromide] and Sulforaphane (SFN) were purchased from Sigma (Saint Louis, MO). The CCK-8 assay kits were purchased from Dojindo, Tokyo, Japan. AlexaFluor488-conjugated IgG was purchased from Invitrogen (Carlsbad, CA). The antibodies anti-NOX4, anti-KEAP1, anti-NRF2, anti-3NT, and anti-NQO1 were purchased from Abcam (Cambridge, MA). Annexin-V/FITC and Propidium Iodide kit was purchased from Nanjing Kaiji Inc., Nanjing, China. ROS assay kits, SOD assay kits, catalase detection kit, and TUNEL kit were purchased from Beyotime Biotechnology, Haimen, China.

Purification of SA3K

The SA3K/pET28 construct was introduced into *Escherichia coli* strain BL21. The purification procedure of SA3K has been previously reported.[30] The purity of recombinant SA3K was examined by SDS-PAGE. Endotoxin concentration was monitored by using a limulus amebocyte kit. Activity was checked by MTT assay with HUVEC cells.

Cell Culture and Procedures

Human corneal epithelial (HCE) cells, simian virus 40 transformed, were obtained from RIKEN Biosource Center, Tokyo, Japan, and were passaged in supplemented hormonal epithelial medium (SHEM), which comprises DMEM-F12 supplemented with 6% heat-inactivated fetal bovine serum, bovine insulin (5 μg/mL), recombinant human epidermal growth factor (10 ng/mL), and 1% penicillin and streptomycin. To establish experimental settings for oxidative stress, H_2O_2 at different concentrations of 0.05 mM, 0.1 mM, and 0.25 mM was added as conditioned medium for treatment of 4 hours, 24 hours, or the time specifically mentioned, respectively; simultaneously, SA3K and other agents were given in the treated groups. For MTT assay and CCK-8 assay experiments, the HCE cells were plated at a density of 1×10^4 cells per well in 96-well culture plates. When the HCE cells were cultured to 70% confluency, the medium was removed and changed in the presence of H_2O_2 or SA3K at a specific concentration and in the absence of H_2O_2 or SA3K. For all other experiments, the HCE cells were plated at a density of 1×10^4 cells per well in 6-well or 24-well culture plates. When the HCE cells were cultured to 70% confluency, the medium was removed and changed in the presence of H_2O_2 or SA3K at a specific concentration and in the absence of H_2O_2 or SA3K. The SFN treatment experiment setting was as follows: when the HCE cells were cultured to 70% confluency, the medium was removed and changed in the presence of SFN or SA3K at specific concentration and in the absence of SFN or SA3K. After treatment for a specified time period, the cells were harvested or prepared for MTT assay/CCK-8 assay, flow cytometry analysis, ROS assay, SOD activity assay, catalase activity assay, fluorescent staining, immunofluoresent staining, Western blot, and quantitative real-time PCR analysis following the methods and procedures described below.

In Vivo Experimental Procedures

The experimental rats were purchased from Shanghai Shilaike Laboratory Animal Co., Ltd., Shanghai, China. The animal experiments were carefully performed in accordance with the ARVO Statement for the Use of Animals in Ophthalmic and Vision Research and the animal experimental protocol was approved by the Animal Experimental Committee of Xiamen University (approval ID: XMUMC2010-03-2).

The animals were kept in the air conditioned facility, with food and water ad libitum.

Wistar rats (male, 180–220 g) were randomly divided into four groups ($n = 5$): (1) control group without any treatment; (2) positive control groups, that is, H_2O_2 plus PBS only group, (3) H_2O_2 plus BSA group, and (4) SA3K treatment group, that is, H_2O_2 plus SA3K group. Two experimental settings were applied from the pilot study. One procedure was as follows: The rats were anesthetized with pentobarbital (50 mg/kg IP), then 10 μL H_2O_2 (500 μM) was topically administered. After 30 minutes, 10 μL PBS only, 10 μL BSA (10 μg in PBS), or 10 μL SA3K (10 μg in PBS) was topically given. After 4 hours, rats were sacrificed, followed by removal and dissection of the eyeballs. The dissected eyeballs were stored in a −80°C freezer for the use of histologic and immunofluorescent staining, fluorescent staining, or Western blot analysis. The other procedure was as follows: The rats were anesthetized with pentobarbital (50 mg/kg IP), then 10 μL H_2O_2 (500 μM) was topically administered. After 30 minutes, 10 μL PBS only, 10 μL BSA (10 μg in PBS), or 10 μL SA3K (10 μg in PBS) was topically given. After 12 hours, 10 μL PBS, 10 μg BSA, or 10 μg SA3K was topically placed again. After 24 hours rats were sacrificed, followed by removal and dissection of the eyeballs. The dissected eyeballs were stored in a −80°C freezer for the use of histologic and immunofluorescent staining, fluorescent staining or Western blot analysis. The dissection of corneal tissue for Western blot was as follows: the whole corneal tissue, including approximately 0.5-mm-width limbal area, was carefully dissected with surgical scissors under a surgical microscope by an experienced person.

MTT Assay/CCK-8 Assay

The cultured HCE cells were used. The MTT assay and CCK-8 assay were conducted with the protocol of the manufacturer. Briefly, after incubation in conditional media for a specified time period, the media was replaced by MTT or CCK-8 constituted in culture media, followed by incubation for 4 hours at 37°C in the dark. For MTT assay, the MTT solution was removed after incubation and the MTT-formazan products were extracted with 100 μL dimethyl sulfoxide in the dark at room temperature, followed by measurement. For the CCK-8 assay, the solution was detected directly after incubation. The absorbance was measured spectrophotometrically at 570 nm with a Bio Tek ELX800 microplate reader (Bio-Tek Instruments, Winooski, VT).

Flow Cytometry Analysis

The cultured HCE cells were used. Twenty-four hours after the treatment of growth medium or the conditioned medium containing H_2O_2 or SA3K, the HCE cells were washed with PBS once, then harvested and stained with the Annexin-V/FITC and Propidium Iodide

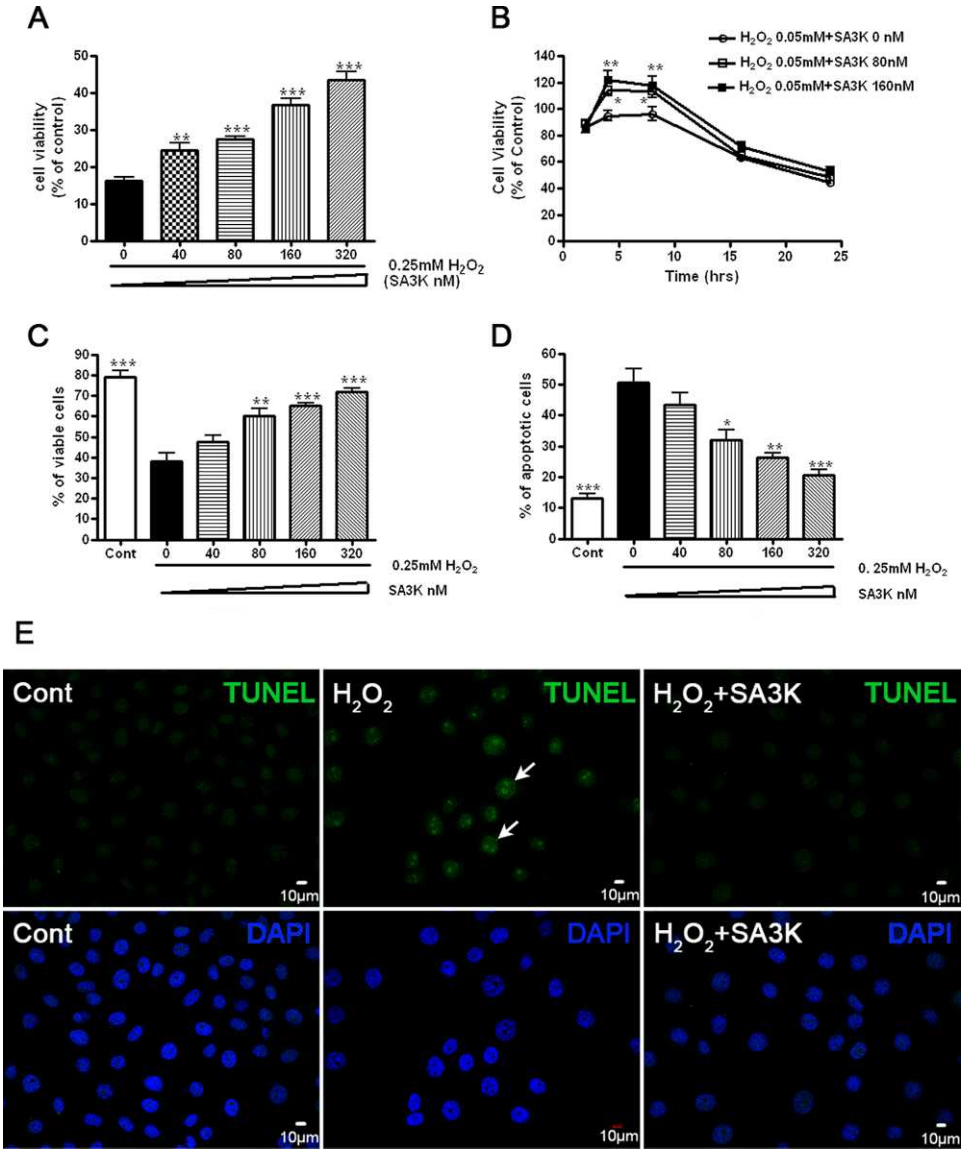

Figure 1. SA3K protected against H_2O_2-induced cell loss in the cultured HCE cells. (**A**) Dose-response: The cell viability was measured in the groups consisting of control, 0.25 mM H_2O_2 only, and 0.25 mM H_2O_2 plus SA3K at concentrations of 40, 80, 160, and 320 nM after treatment of 24 hours (mean ± SEM, $n = 5$, $^{**}P < 0.01$; $^{***}P < 0.001$ versus H_2O_2-only group). (**B**) Time-course: The cell viability was measured in the groups consisting of control, 0.05 mM H_2O_2 only, and 0.05 mM H_2O_2 plus SA3K at concentrations of 80 and 160 nM at the time points of 2, 4, 8, 16 and 24 hours after treatment with H_2O_2 and SA3K (mean ± SEM, $n = 5$, $^{*}P < 0.05$; $^{**}P < 0.01$ versus H_2O_2-only group). (**C**, **D**) In flow cytometry assay, the viable cells (**C**) and the number of apoptotic cells (**D**) were measured in the groups consisting of control, 0.25 mM H_2O_2 only, and 0.25 mM H_2O_2 plus SA3K at concentrations of 40, 80, 160, and 320 nM after treatment of 24 hours (mean ± SEM, $n = 4$, $^{*}P < 0.05$; $^{**}P < 0.01$; $^{***}P < 0.001$ versus H_2O_2-only group). (**E**) The representative TUNEL fluorescent images for the groups consisting of control, 0.1 mM H_2O_2 only, and 0.1 mM H_2O_2 plus 160 nM SA3K after treatment of 24 hours in the cultured HCE cells (green: TUNEL-positive staining (*arrows*); blue: DAPI nuclear staining).

by using the kit and following the protocol recommended by the manufacturer. The apoptotic cells were measured from the flow cytometry profile.[31] The samples were analyzed to quantify apoptotic cells and cell viability by flow cytometry.

ROS Assay

The cultured HCE cells were used. ROS levels were measured by following the protocol of the manufacturer. Briefly, changes in intracellular ROS levels were determined by measuring the oxidative conversion of cell permeable 2′,7′-dichlorofluorescein diacetate (DCFH-DA) to fluorescent dichlorofluorescein (DCF). Cells in 24-well culture dishes were washed once with PBS and then were incubated with DCFH-DA at 37°C for 30 minutes. DCF fluorescence distribution of 5000 cells was detected by flow cytometric analysis at an excitation wavelength of 488 nm and at an emission wavelength of 525 nm.

SOD Activity Assay

The cultured HCE cells were used. SOD activity was measured by following the protocol of the manufacturer. Briefly, it measured the formation of a formazan dye upon reduction of the tetrazolium salt WST-1 (2-(4-iodophenyl)-3-(4-nitrophenyl)-5-(2,4-disulfophenyl)-2H-tet-

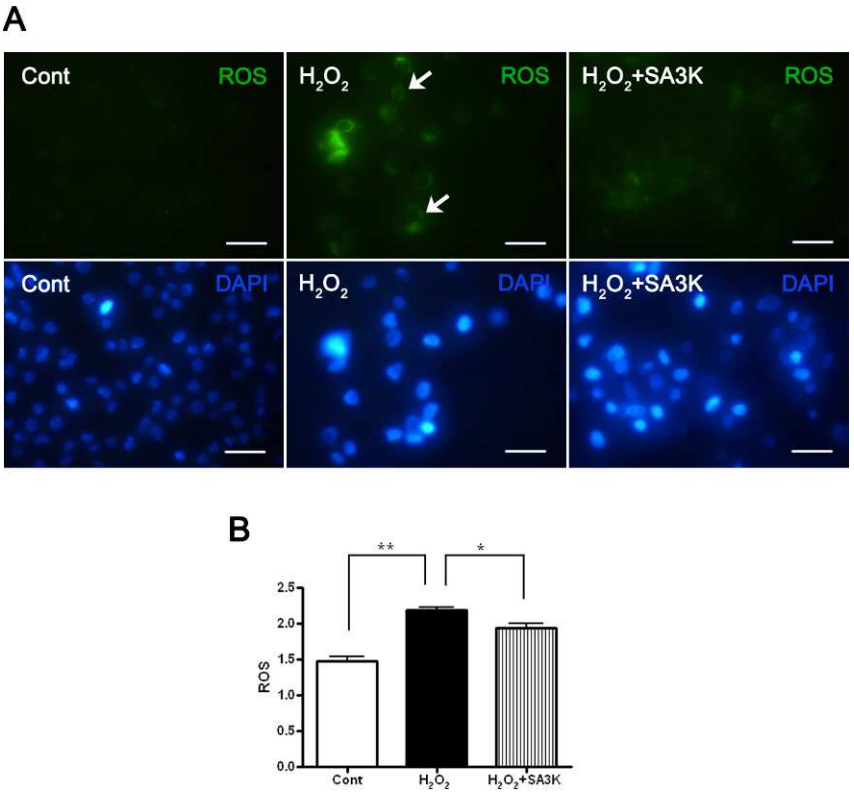

Figure 2. SA3K suppressed the ROS production in the cultured HCE cells. (**A**) Representative autofluorescent images in the groups consisting of control, 0.25 mM H_2O_2 only, and 0.25 mM H_2O_2 plus 80 nM SA3K after treatment of 24 hours in the cultured HCE cells. Green represents autofluorescent intracellular ROS expression; blue represents DAPI nuclear staining (scale bar: 50 μm). (**B**) ROS production was detected by fluorescent DCF assay in the groups consisting of control, 0.25 mM H_2O_2 only, and 0.25 mM H_2O_2 plus 80 nM SA3K after treatment of 24 hours in the cultured HCE cells (mean ± SEM, $n = 3$, $^*P < 0.05$; $^{**}P < 0.01$).

razolium) with superoxide anions. This mixture of the supernatant and enzyme working solution was incubated for 20 minutes at 37°C and the absorbance was read at 450 nm. For the data analysis, the activity was calculated in units and was divided by the amount of protein measured.

Catalase Activity Assay

The cultured HCE cells were used. Catalase activity was detected by following the protocol of the manufacturer. The colorimetric method

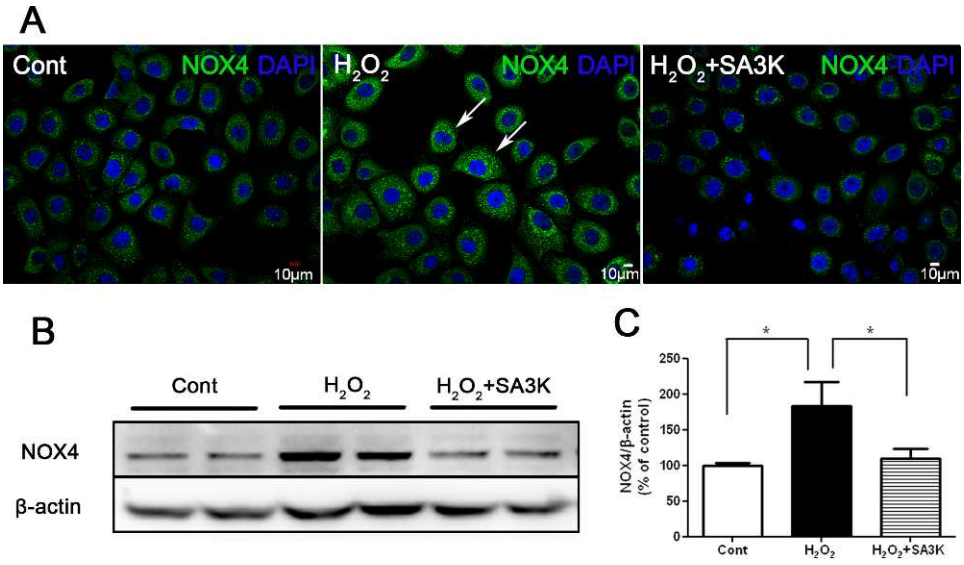

Figure 3. SA3K inhibited the ROS-generating factor NOX4. (**A**) The representative immunofluorescent staining images of anti-NOX4 antibody (green color [*arrows*]) in the groups consisting of control, 0.1 mM H_2O_2 only, and 0.1 mM H_2O_2 plus 80 nM SA3K after treatment of 4 hours in the cultured HCE cells. (**B**) The representative Western blot images of NOX4, with the order of gel bands from left to right individually: 1–2, control; 3–4, 0.1 mM H_2O_2 only; and 5–6, 0.1 mM H_2O_2 plus 80 nM SA3K after treatment of 4 hours. (**C**) The statistical analysis of Western blot results for NOX4 (mean ± SEM, $n = 3$–4, $^*P < 0.05$).

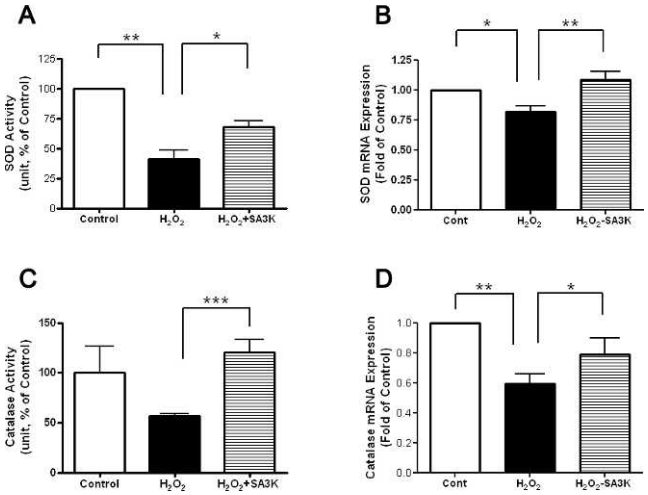

Figure 4. SA3K upregulated the ROS-degrading factors SOD and catalase. (**A**) SOD activity was measured by the SOD assay kit in the groups consisting of control, 0.25 mM H_2O_2 only, and 0.25 mM H_2O_2 plus 80 nM SA3K after treatment of 24 hours (mean ± SEM, $n = 3$, $^*P < 0.05$; $^{**}P < 0.01$). (**B**) Quantitative RT-PCR (qRT-PCR) of *SOD2* gene expression was measured in the groups consisting of control, 0.1 mM H_2O_2 only, and 0.1 mM H_2O_2 plus 80 nM SA3K after treatment of 24 hours (mean ± SEM, $n = 5$, $^*P < 0.05$; $^{**}P < 0.01$). (**C**) Catalase (CAT) activity was detected in the groups consisting of control, 0.25 mM H_2O_2 only, and 0.25 mM H_2O_2 plus 80 nM SA3K after treatment of 24 hours in the cultured HCE cells (mean ± SEM, $n = 3$, $^{***}P < 0.001$). (**D**) qRT-PCR of *CAT* gene expression was measured in the groups consisting of control, 0.1 mM H_2O_2 only, and 0.1 mM H_2O_2 plus 80 nM SA3K after treatment of 24 hours in the cultured HCE cells (mean ± SEM, $n = 5$, $^*P < 0.05$; $^{**}P < 0.01$).

has been described previously.[32] For the data analysis, the activity was calculated in units and was divided by the amount of protein measured.

Autofluorescent Assay and Immunofluorescent Staining

After the HCE cells were incubated for the ROS assay for 30 minutes, the autofluorescent ROS expression of cells was detected by a laser fluorescent microscope and the photographic images were taken.

For the immunofluorescent staining with anti-3NT, anti-NOX4, anti-KEAP1, and anti-NRF2 antibodies, the HCE cells were fixed in 4% paraformaldehyde for 2 hours and then kept in 70% ethanol for use. The HCE cells or the corneal sections were incubated with anti-3NT antibody (1:400), anti-NOX4 antibody (1:400), anti-KEAP1 antibody, (1:400) and anti-NRF2 antibody (1:400) at 4°C overnight. After further incubation in AlexaFluor488-conjugated IgG (1:1000), sections were counterstained with 4,6-diamino-2-phenylindole (DAPI), mounted, and photographed by using a confocal laser scanning microscope (Fluoview 1000; Olympus, Tokyo, Japan).

TUNEL fluorescent staining was conducted by following the protocol of the manufacturer.

Western Blot

Total cellular proteins of the harvested HCE cells or dissected corneal tissues were extracted. The standard Western blot assay protocol was applied. The specific primary antibodies anti-3-NT, anti-NOX4, anti-NRF2, and anti-NQO1, and a horseradish peroxidase–conjugated secondary antibody, were used. Finally, the specific bands were visualized by enhanced chemiluminescence reagents and recorded on film. The subcellular fractions including cytoplasmic, nuclear, and membrane fractions were separated and prepared from the corneal tissues; each fraction was identified by the markers; and then anti-NRF2 in the nuclear fraction was examined by Western blot analysis.

RNA Isolation and Quantitative RT-PCR

Total RNA was extracted from the cultured HCE cells by using TRIzol reagent (Invitrogen). Reverse transcription was performed with Oligo 18T primers and reverse transcription reagents according to the manufacturer's protocol (TaKaRa, Shiga, Japan). Quantitative real-time PCR was performed with mRNA special primers. The following primers were used for the PCR: for *SOD2*, 5′-GAGAAGTACCAGGAGGCGTTG-3′ (forward) and 5′-GAGCCTTGGACACCAACAGAT-3′ (reverse); for catalase, 5′-ACTGAGGTCCACCCTGACTAC-3′ (forward) and 5′-TCGCATTCTTAGGCTTCTCA-3′ (reverse); for *GSTP*, 5′-GCTCTATGGGAAGGACCAG-3′ (forward) and 5′-CTCAAAAGGCTTCAGTTGC-3′ (reverse). PCR reactions were performed on a BIO-RAD CFX-96 Real Time system with SYBR Premix Ex Taq (TaKaRa) at 95°C for 10 minutes, followed by 45 cycles of 95°C for 10 seconds, 57°C for 30 seconds, and 75°C for 10 seconds, after which melt curve analysis was performed at once from 65°C to 95°C. All reactions were performed in triplicate and the average Ct values greater than 38 were treated as negative.

Statistical Analysis

One-way analysis of variance test was conducted to analyze the data from MTT/CCK-8 assay, flow cytometry, ROS assay, SOD activity assay, catalase activity assay, Western blot, and quantitative real-time PCR, followed by a post hoc analysis Tukey test to compare the differences between the groups or a Student's *t*-test. $P < 0.05$ was considered statistically significant.

Results

SA3K Protected against H_2O_2-Induced Cell Loss in Cultured HCE Cells

To determine if SA3K has protective effects against oxidative stress, we used H_2O_2 as an oxidative stressor. Briefly, cultured HCE cells were exposed to the medium containing H_2O_2 for a specified time period. As shown by the measurement of cell viability with the MTT assay, the number of viable HCE cells was significantly decreased after exposure to 0.25 mM H_2O_2 for 24 hours, as compared with the control group. SA3K at concentrations of 40, 80, 160 and 320 nM increased the cell viability of cultured HCE cells treated by H_2O_2 in a concentration-dependent manner (Fig. 1A). In another separate experiment of the HCE cell viability measured by CCK-8 assay, SA3K at concentrations of 80 and 160 nM increased the cell viability of the HCE cells in a time-dependent manner after exposure to H_2O_2 at a concentration of 0.05 mM at time points of 2, 4, 8, 16, and 24 hours, with statistically significant changes at time points of 4 and 8 hours (Fig. 1B).

To further confirm the protective effects of SA3K against H_2O_2 induction, we also conducted flow cytometry detection and TUNEL fluorescent staining to quantify dead cells among the cultured HCE cells. We demonstrated that SA3K at concentrations of 40, 80, 160, and 320 nM increased the number of viable cells and decreased the number of apoptotic cells induced by 0.25 mM H_2O_2 after 24-hour treatment in a concentration-dependent manner (Figs. 1C, 1D). On the other hand, in another separate experiment, SA3K at a concentration of 160 nM decreased the number of TUNEL positive–staining cells induced by 0.1 mM H_2O_2 after 24-hour treatment (Fig. 1E). Taken together, these results suggest that SA3K protects the HCE cells and reduces cell death caused by oxidative stress induced by H_2O_2.

SA3K Suppressed the Production of ROS

To examine the level of ROS in the oxidative stress setting that we established and the effects of SA3K, we measured both the

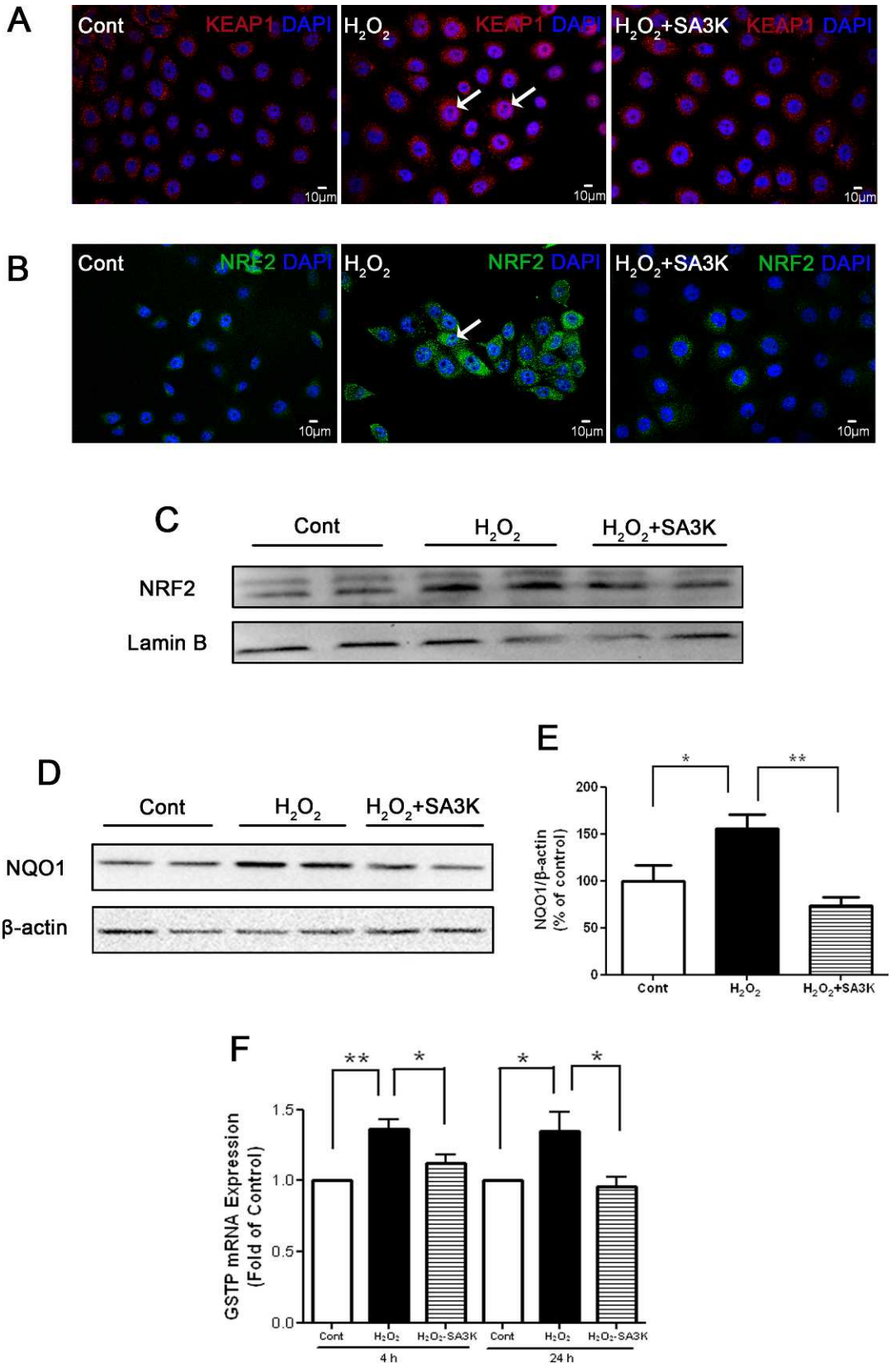

FIGURE 5. SA3K modulated the KEAP1-NRF2 pathway. (**A**) The representative immunofluorescent staining images of anti-KEAP1 antibody (red color) in the groups consisting of control, 0.1 mM H_2O_2 only, and 0.1 mM H_2O_2 plus 160 nM SA3K after treatment of 24 hours in the cultured HCE cells. Blue color represents DAPI staining of nucleus. The *arrows* indicate nuclear translocation of KEAP1. (**B**) The representative immunofluorescent staining images of anti-NRF2 antibody (green color) in the groups consisting of control, 0.1 mM H_2O_2 only, and 0.1 mM H_2O_2 plus 80 nM SA3K after treatment of 24 hours in the cultured HCE cells. Blue color represents DAPI staining of nucleus. The arrows indicate expression of NRF2. (**C**) The representative Western blot images of NFR2 in the nuclear fraction, with the order of gel bands from left to right individually: 1–2, control; 3–4, 0.1 mM H_2O_2 only; and 5–6, 0.1 mM H_2O_2 plus 80 nM SA3K after treatment of 24 hours. (**D**) The representative Western blot images of NQO1, with the order of gel bands from left to right individually: 1–2, control; 3–4, 0.1 mM H_2O_2 only; and 5–6, 0.1 mM H_2O_2 plus 80 nM SA3K after treatment of 24 hours. (**E**) The statistical analysis of Western blot results for NQO1 (mean ± SEM, $n = 4$, $^*P < 0.05$). (**F**) The qRT-PCR results of gene expression of *GSTP* in the groups consisting of control, 0.1 mM H_2O_2 only, and 0.1 mM H_2O_2 plus 80 nM SA3K after treatment of 4 and 24 hours in the cultured HCE cells (mean ± SEM, $n = 4$–5, $^*P < 0.05$; $^{**}P < 0.01$).

generation of ROS by autofluorescent image detection and the quantification of ROS production. An exposure to H_2O_2 at a concentration of 0.25 mM for 24 hours resulted in high levels of ROS as shown by examination of the autofluorescent image (Fig. 2A, green color, as arrow indicates), whereas SA3K at a concentration of 80 nM significantly suppressed the production of ROS, indicating the antioxidant effect of SA3K (Fig. 2A). In a consistent result, a different quantitative measurement showed that ROS production was significantly increased in the H_2O_2-treated group (0.1 mM, 24 hours) as compared to the control group (Fig. 2B). Meanwhile, SA3K at a concentration of 80 nM significantly blocked the production of ROS (Fig. 2B), suggesting that SA3K suppressed ROS production under the oxidative stress induced by H_2O_2.

SA3K Inhibited an Oxidant Enzyme

To investigate the mechanism underlying the antioxidant effect of SA3K, we focused on the system of ROS generation and ROS degradation. NOX4 is an isoform of NADPH oxidase, which is well recognized as the main factor of ROS generation. We examined the expression of NOX4 in the oxidative stress model induced by H_2O_2 and the effects of SA3K by using immunofluorescent staining and Western blot analysis with an anti-NOX4 antibody.

As shown by the immunofluorescent staining, an exposure to H_2O_2 at a concentration of 0.1 mM for 4 hours resulted in a strong expression of NOX4 in the cytoplasm as well as the nuclear membranes of the cultured HCE cells, while SA3K at a concentration of 80 nM suppressed the expression of NOX4 in HCE cells after exposure to H_2O_2 (Fig. 3A, green color represents the anti-NOX4 antibody staining). In the same experimental setting with the induction of H_2O_2 in the cultured HCE cells, Western blot results demonstrated that the protein level of NOX4 increased after exposure to 0.1 mM H_2O_2 for 4 hours, while SA3K at a concentration of 80 nM significantly reduced the level of NOX4 induced by H_2O_2 (Figs. 3B, 3C).

SA3K Upregulated ROS Degradation

It is well documented that there are several ROS-degrading or antioxidant enzymes in cells, such as SOD and catalase. To determine if SA3K targets ROS degradation, we measured the enzyme activities and gene expression of SOD and catalase in the H_2O_2-induced oxidative stress setting.

It was revealed that the SOD activity of the cultured HCE cells was significantly reduced in the H_2O_2-treated group at a concentration of 0.25 mM after 24-hour treatment, as compared to the control group; meanwhile, SA3K at a concentration of 80 nM significantly increased SOD activity in the cells after exposure to H_2O_2 (Fig. 4A). On the other hand, in a separate experiment with quantitative real-time PCR assay, gene expression of *SOD2* in the HCE cells was significantly downregulated after exposure to 0.1 mM H_2O_2 for 24 hours, while SA3K at a concentration of 80 nM upregulated the gene expression of *SOD2* (Fig. 4B).

In addition, the catalase activity assay showed that catalase activity was decreased in the group after exposure to H_2O_2 at a concentration of 0.25 mM for 24 hours, while SA3K at a concentration of 80 nM significantly upregulated the catalase activity induced by H_2O_2 (Fig. 4C). Quantitative real-time PCR assay also showed that the gene expression of catalase in the cultured HCE cells was significantly inhibited after exposure to 0.1 mM H_2O_2 for 24 hours, whereas SA3K at a concentration of 80 nM significantly upregulated the gene expression of catalase (Fig. 4D).

These above experimental results suggested that SA3K targets the ROS generation/degradation systems by suppressing ROS generation while upregulating the activity of ROS degradation/antioxidant enzymes.

SA3K Modulated the KEAP1-NRF2 Pathway

To further investigate the mechanism underlying the antioxidant activity of SA3K, we evaluated the effect of SA3K on the KEAP1/NRF2 pathway—which is believed to play important roles in modulating the redox system—by measuring the key components of the KEAP1-NRF2-ARE pathway at the protein level and gene expression level.

Immunofluorescent staining with the anti-KEAP1 antibody showed that exposure to H_2O_2 (0.1 mM, 24 hours) resulted in an intensive immunosignal of KEAP1 in the cytoplasm as well as the nucleus of HCE cells (Fig. 5A), indicating that KEAP1 was activated by treatment with H_2O_2, which was followed by nuclear translocation of KEAP1. Meanwhile, SA3K at a concentration of 160 nM suppressed the immunosignals of KEAP1 both in the cytoplasm and the nucleus (Fig. 5A, red color for KEAP1 staining, blue color for DAPI nuclear staining).

Immunofluorescent staining using the anti-NRF2 antibody showed that exposure to H_2O_2 (0.1 mM, 24 hours) substantially increased intensity of NRF2 staining in the cultured HCE cells; SA3K at a concentration of 80 nM inhibited the expression of NRF2 (Fig. 5B, green color for NRF2 staining, blue color for DAPI nuclear staining). Interestingly, Western blot analysis of the nuclear fraction, using the anti-NRF2 antibody, revealed that the NRF2 level in the nucleus was elevated in the H_2O_2-treated HCE cells (0.1 mM, 24 hours), whereas SA3K at 80 nM downregulated the NRF2 level in the nucleus of the HCE cells after exposure to H_2O_2 (Fig. 5C).

In addition, we also found through Western blot analysis that the level of NQO1, a key downstream factor of the KEAP1-NFR2-ARE pathway, was significantly increased after exposure to H_2O_2 (0.1 mM, 24 hours), while SA3K at a concentration of 80 nM suppressed the NQO1 level after treatment of H_2O_2 (Figs. 5D, 5E).

To examine the gene expression alteration regulated by the KEAP1-NRF2 pathway, we measured the gene expression of *GSTP*, which is considered to be a key downstream component of the KEAP1-NRF2 pathway or of phase 2 of the ARE family, by

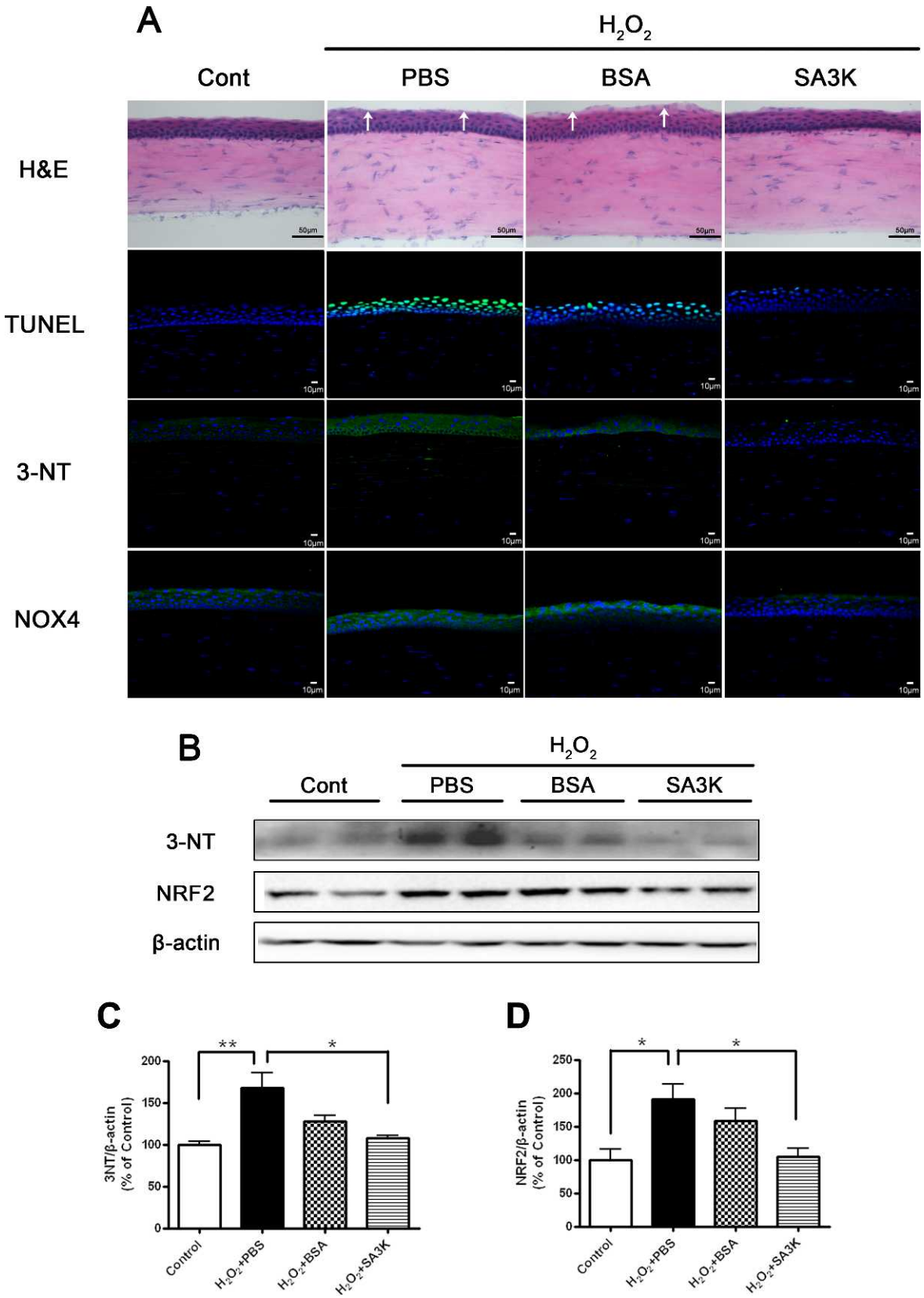

Figure 6. SA3K had antioxidant effects in in vivo rat corneal epithelium. (**A**) Representative images (*from the upper row to the bottom row*) of H&E staining, fluorescence staining of TUNEL, and immunofluorescence staining with anti-3NT antibody and anti-NOX4 antibody. The images from the *left column* to the *right column* are from the control group without any treatment, H_2O_2 (500 μM, 10 μL) plus PBS group, H_2O_2 (500 μM, 10 μL) plus BSA (20 μg/eye/day) group, and H_2O_2 (500 μM, 10 μL) plus SA3K (20 μg/eye/day) group. The treatment time was 24 hours. The *arrows* indicate mild rough surface, mildly damaged corneal epithelium (scale bar of H&E staining: 50 μm; all other scale bars: 10 μm). (**B**) Representative images of anti-3NT antibody and anti-NRF2 antibody Western blot results, with the order of gel bands from left to right individually: 1–2, control

group without any treatment; 3–4, H_2O_2 (500 μM, 10 μL) plus PBS group; 5–6, H_2O_2 (500 μM, 10 μL) plus BSA (10 μg/eye) group; and 7–8, H_2O_2 (500 μM, 10 μL) plus SA3K (10 μg/eye) group. The treatment time was 4 hours. Each band represents an individual rat corneal sample. (**C**, **D**) Statistical analysis of anti-3NT antibody and anti-NRF2 antibody Western blot results, respectively (mean ± SEM, $n = 3$, $^*P < 0.05$; $^{**}P < 0.01$).

quantitative real-time PCR assay. Exposure to 0.1 mM H_2O_2, as an inducer to activate the KEAP1-NRF2 pathway, resulted in the upregulation of gene expression of *GSTP* in the cultured HCE cells at time points of 4 and 24 hours, whereas SA3K at a concentration of 80 nM significantly inhibited the gene expression of *GSTP* induced by H_2O_2 (Fig. 5F).

To further elucidate the mechanism of how SA3K mediates NRF2, we established treatment with SFN and selected the concentration of 10 μM SFN in cultured HCE cells after a pilot study. SFN is an inhibitor of KEAP1 and can disassociate the KEAP1-NRF2 complex, which eventually results in the accumulation of NRF2 in cells.[20] It was demonstrated that treatment with 10 μM SFN for 24 hours decreased cell viability significantly (see Supplementary Material and Supplementary Fig. S1A, http://www.iovs.org/lookup/suppl/doi:10.1167/iovs.12-9729/-/DCSupplemental); SFN also increased TUNEL-positive staining (see Supplementary Material and Supplementary Fig. S1B, http://www.iovs.org/lookup/suppl/doi:10.1167/iovs.12-9729/-/DCSupplemental). Meanwhile, SFN elevated NRF2 immunosignals (see Supplementary Material and Supplementary Fig. S1C, http://www.iovs.org/lookup/suppl/doi:10.1167/iovs.12-9729/-/DCSupplemental), suggesting that SFN may induce the accumulation of NRF2 and eventually lead to cell death. Interestingly, SA3K at 160 nM significantly reduced cell death after treatment with SFN (see Supplementary Material and Supplementary Figs. S1A, S1B, http://www.iovs.org/lookup/suppl/doi:10.1167/iovs.12-9729/-/DCSupplemental); in addition, SA3K decreased NRF2 accumulation after treatment with SFN (see Supplementary Material and Supplementary Fig. S1C, http://www.iovs.org/lookup/suppl/doi:10.1167/iovs.12-9729/-/DCSupplemental). It was suggested that SA3K might inhibit the accumulation of NRF2 and protect the HCE cells.

Taken together, these results suggest that the KEAP1-NRF2 pathway is activated by H_2O_2, whereas SA3K blocks H_2O_2-induced activation of the KEAP1-NRF2 pathway by suppressing the protein level or gene expression of NRF2, as well as the downstream factors of the KEAP1-NRF2-ARE pathway, NQO1 and GSTP.

SA3K Had Antioxidant Effects in the Rat Corneal Epithelium

To examine the antioxidant effect of SA3K on the corneal epithelium and the mechanism of SA3K in in vivo conditions, we established an oxidative stress setting by topical administration of 500 μM H_2O_2 to rat eyes. The histologic staining, immunostaining, and Western blot analysis were conducted after 4 and 24 hours.

The histologic hematoxylin and eosin (H&E) staining showed that the surface of the corneal epithelium layer was mildly damaged and the thickness of the stroma layer was increased after treatment with 500 μM H_2O_2 for 24 hours, but no significant damage or inflammation was observed; on the other hand, SA3K at 20 μg/eye/day ameliorated this mild damage in the corneal epithelial layer (Fig. 6A, the top row of images, arrows indicate mildly damaged surface). It was also revealed that TUNEL positive–staining cells in the corneal epithelium increased after exposed to H_2O_2, while SA3K at 20 μg/eye/day decreased the number of TUNEL-positive cells, suggesting that SA3K alleviated cell death induced by oxidative stress in rat corneal epithelium (Fig. 6A, the second row of images). In addition, immunofluorescence staining using the anti-3NT antibody, a widely used marker of oxidative stress, showed that the level of 3-NT was increased in the corneal epithelium after exposure to H_2O_2, while SA3K at 20 μg/eye/day suppressed 3-NT expression, indicating that SA3K has an antioxidant effect on the corneal epithelium in vivo (Fig. 6A, the third row of images). Furthermore, the immunofluorescence staining of anti-NOX4 antibody also revealed that the level of NOX4 was increased in the corneal epithelium after exposure to H_2O_2, while SA3K at 20 μg/eye/day inhibited the NOX4 expression, suggesting that SA3K suppressed the generation of oxidative stress (Fig. 6A, the bottom row of images).

To further confirm the ROS expression changes and to study the mechanism of SA3K on ROS pathway in rat corneal epithelium, we conducted Western blot analysis with the anti-3NT and anti-NRF2 antibodies. It was demonstrated that the level of 3-NT in the rat cornea was significantly upregulated after exposure to 500 μM H_2O_2 for 4 hours, while SA3K at 10 μg/eye significantly suppressed the 3-NT level (Figs. 6B, 6C), suggesting that SA3K inhibited the production of ROS in the in vivo model. In addition, the level of NRF2 in the rat cornea was significantly increased after exposure to H_2O_2, while SA3K at 10 μg/eye significantly downregulated the NRF2 level (Figs. 6B, 6D), indicating that SA3K suppressed the key factor of the KEAP1-NRF2 pathway after induction of H_2O_2.

Collectively, in the in vivo oxidative stress setting, SA3K also had protective effects on the rat corneal epithelium against oxidative stress by inhibiting the generation of ROS and modulating the KEAP1-NRF2 pathway. These results are consistent with those from the cultured HCE cells.

Discussion

SA3K is a serine proteinase inhibitor. We recently demonstrated that SA3K has antiangiogenesis and anti-inflammatory activity in corneal injury models.[28] In this study we showed for the first time that SA3K has antioxidant effects in the corneal epithelium. Furthermore, we found that these antioxidant effects are exerted through the mediation of ROS generation/degradation and the KEAP1-NRF2 pathway. These studies indicated that SA3K is a novel antioxidant factor in the SERPIN family. These findings will contribute to our understanding of endogenous antioxidant systems and to the development of new therapeutic agents for the oxidative stress-related corneal diseases.

Oxidative stress is a very complex process and involves multiple factors or pathways, such as NOX4 and the KEAP1-NRF2 pathway. Our study suggested that SA3K can target the ROS system, restore the balance of ROS generation and degradation, modulate the KEAP1-NRF2 pathway, and play an antioxidant role.

It is believed that NRF2 is an important transcription factor and plays a key role in the ROS signaling pathway.[18–20] NRF2 is regulated by KEAP1 and forms a KEAP1-NRF2 complex. KEAP1 binds with Cul3-containing E3 ubiquitin ligase.[24] Under oxidative stress (e.g., exposure to H_2O_2), the Cul3-containing E3 ubiquitin ligase is inhibited, subsequently leading to NRF2 accumulation in the cytoplasm and translocation in the nucleus, as well as activation of ARE-dependent genes, such as *NQO1* and *GSTP*.[20,21] In the present study, H_2O_2 induced the expression of KEAP1 in the cytoplasm and nucleus as well as the nuclear translocation of NRF2, followed by activation of NQO1 and GSTP; interestingly, SA3K suppressed the battery of

activities induced by oxidative stress, suggesting that SA3K blocks the early stage of H_2O_2-induced activation of the KEAP-NRF2 pathway, inhibits the subsequent activity of the downstream pathway, and restores the balance of the KEAP1-NRF2-ARE pathway from excess levels. The excess accumulation of NRF2 in the cell is considered to be a factor that induces apoptosis and eventually leads to cell protection against oxidative stress.[20,21] As revealed in Figure S1 (see Supplementary Material and Supplementary Fig. S1, http://www.iovs.org/lookup/suppl/doi:10.1167/iovs.12-9729/-/DCSupplemental), it was suggested that SA3K might inhibit the accumulation of NRF2 and protect the HCE cells. We showed that SA3K targets the KEAP1-NRF2 pathway, but further elucidation of the detailed mechanism of SA3K on the KEAP1-NRF2 pathway is needed, including the binding site of the KEAP1-NRF2 complex by SA3K, the interaction between the KEAP1-NRF2-ARE pathway and other signaling pathways, and indirect actions of SA3K on the KEAP1-NRF2-ARE pathway.

We applied an oxidative stress setting in an in vivo condition and suggested that SA3K's antioxidant activity was mediated through the important factors of ROS generation/degradation systems and pathways, such as NOX4 and NRF2. It will be helpful to further identify the genetic pathogenesis of corneal oxidative stress by using suitable and available ROS transgenic animal models, such as transgenic (Tg-SOD) mice.[33]

In our in vivo model, H_2O_2 may induce the loss of the epithelial barrier function, which then leads to stroma swelling. SA3K ameliorated H_2O_2-induced minor injury of epithelium surface, but did not improve the thickness or swelling of the stroma, suggesting that SA3K may not be able to protect from the dysfunction of epithelial barrier induced by H_2O_2.

We have previously reported that SA3K blocks the Wnt signaling pathway, which represents a unifying mechanism for its anti-inflammatory, antiangiogenic, and antifibrotic activities.[29] It remains to be investigated whether SA3K's antioxidant activity in the corneal epithelium is through modulation of the Wnt pathway.[34,35]

It is known that oxidative stress is the pathogenesis underlying various ocular diseases, including Fuchs' endothelial corneal dystrophy,[7–9] keratoconus, and others.[10] This study may contribute to better understanding of the oxidative stress state in corneal epithelium cells and reveal a new target for pharmacologic intervention and new antioxidants in the treatment of corneal diseases.

References

1. Wasserman WW, Fahl WE. Functional antioxidant responsive elements. *Proc Natl Acad Sci U S A*. 1997;94:5361–5366.
2. Kietzmann T. Intracellular redox compartments: mechanisms and significances. *Antioxid Redox Signal*. 2010;13:395–398.
3. Giacco F, Brownlee M. Oxidative stress and diabetic complications. *Circ Res*. 2010;107:1058–1070.
4. Khandhadia S, Lotery A. Oxidation and age-related macular degeneration: insights from molecular biology. *Expert Rev Mol Med*. 2010;12:e34.
5. Melov S. Animal models of oxidative stress, aging, and therapeutic antioxidant interventions. *Int J Biochem Cell Biol*. 2002;34:1395–1400.
6. Buddi R, Lin B, Atilano SR, et al. Evidence of oxidative stress in human corneal diseases. *J Histochem Cytochem*. 2002;50:341–351.
7. Azizi B, Ziaei A, Fuchsluger T, et al. p53-regulated increase in oxidative-stress—induced apoptosis in Fuchs endothelial corneal dystrophy: a native tissue model. *Invest Ophthalmol Vis Sci*. 2011;52:9291–9297.
8. Jurkunas UV, Bitar MS, Funaki T, et al. Evidence of oxidative stress in the pathogenesis of fuchs endothelial corneal dystrophy. *Am J Pathol*. 2010;177:2278–2289.
9. Jurkunas UV, Rawe I, Bitar MS, et al. Decreased expression of peroxiredoxins in Fuchs' endothelial dystrophy. *Invest Ophthalmol Vis Sci*. 2008;49:2956–2963.
10. Shoham A, Hadziahmetovic M, Dunaief JL, et al. Oxidative stress in diseases of the human cornea. *Free Radic Biol Med*. 2008;45:1047–1055.
11. Bedard K, Krause KH. The NOX family of ROS-generating NADPH oxidases: physiology and pathophysiology. *Physiol Rev*. 2007;87:245–313.
12. Frey RS, Ushio-Fukai M, Malik AB. NADPH oxidase-dependent signaling in endothelial cells: role in physiology and pathophysiology. *Antioxid Redox Signal*. 2009;11:791–810.
13. Ushio-Fukai M. Redox signaling in angiogenesis: role of NADPH oxidase. *Cardiovasc Res*. 2006;71:226–235.
14. Petry A, Weitnauer M, Görlach A. Receptor activation of NADPH oxidases. *Antioxid Redox Signal*. 2010;13:467–487.
15. Petry A, Djordjevic T, Weitnauer M, Kietzmann T, Hess J, Görlach A. NOX2 and NOX4 mediate proliferative response in endothelial cells. *Antioxid Redox Signal*. 2006;8:1473–1484.
16. Block K, Gorin Y, Abboud HE. Subcellular localization of Nox4 and regulation in diabetes. *Proc Natl Acad Sci U S A*. 2009;106:14385–14390.
17. Geiszt M, Leto TL. The Nox family of NAD(P)H oxidases: host defense and beyond. *J Biol Chem*. 2004;279:51715–51718.
18. Li W, Kong AN. Molecular mechanisms of Nrf2-mediated antioxidant response. *Mol Carcinog*. 2009;48:91–104.
19. Nguyen T, Nioi P, Pickett CB. The Nrf2-antioxidant response element signaling pathway and its activation by oxidative stress. *J Biol Chem*. 2009;284:13291–13295.
20. Kaspar JW, Niture SK, Jaiswal AK. Nrf2:INrf2 (Keap1) signaling in oxidative stress. *Free Radic Biol Med*. 2009;47:1304–1309.
21. Kensler TW, Wakabayashi N. Nrf2: friend or foe for chemoprevention? *Carcinogenesis*. 2010;31:90–99.
22. Dinkova-Kostova AT, Talalay P. NAD(P)H: quinone acceptor oxidoreductase 1 (NQO1), a multifunctional antioxidant enzyme and exceptionally versatile cytoprotector. *Arch Biochem Biophys*. 2010;501:116–123.
23. Jaiswal AK. Nrf2 signaling in coordinated activation of antioxidant gene expression. *Free Radic Biol Med*. 2004;36:1199–1207.
24. Kaspar JW, Jaiswal AK. An autoregulatory loop between Nrf2 and Cul3-Rbx1 controls their cellular abundance. *J Biol Chem*. 2010;285:21349–21358.
25. Chai KX, Ma JX, Murray SR, Chao J, Chao L. Molecular cloning and analysis of the rat kallikrein-binding protein gene. *J Biol Chem*. 1991;266:16029–16036.
26. Gao G, Shao C, Zhang SX, et al. Kallikrein-binding protein: a novel angiogenic inhibitor of the serpin family. *Diabetologia*. 2003;46:689–698.
27. Zhang B, Hu Y, Ma JX. Anti-inflammatory and antioxidant effects of SERPINA3K in the retina. *Invest Ophthalmol Vis Sci*. 2009;50:3943–3952.
28. Zhang B, Ma JX. SERPINA3K prevents oxidative stress induced necrotic cell death by inhibiting calcium overload. *PLoS ONE*. 2008;3:e4077.
29. Zhang B, Abreu JG, Zhou K, et al. Blocking the Wnt pathway, a unifying mechanism for an angiogenic inhibitor in the serine proteinase inhibitor family. *Proc Natl Acad Sci U S A*. 2010;107:6900–6905.
30. Liu X, Lin Z, Zhou T, et al. Anti-angiogenic and anti-inflammatory effects of SERPINA3K on corneal injury. *PLoS ONE*. 2011;6:e16712.

31. Zhou Y, Liu Q, Zhou T, et al. Modulation of the canonical Wnt pathway by Benzalkonium Chloride in corneal epithelium. *Exp Eye Res*. 2011;93:355–362.
32. Góth L. A simple method for determination of serum catalase activity and revision of reference range. *Clin Chim Acta*. 1991; 196:143–152.
33. Pouyet L, Carrier A. Mutant mouse models of oxidative stress. *Transgenic Res*. 2010;19:155–164.
34. Korswagen HC. Regulation of the Wnt/beta-catenin pathway by redox signaling. *Dev Cell*. 2006;10:687–688.
35. Zhou T, Zhou KK, Lee K, et al. The role of lipid peroxidation products and oxidative stress in activation of the canonical wingless-type MMTV integration site (WNT) pathway in a rat model of diabetic retinopathy. *Diabetologia*. 2011;54:459–468.